Leaf Area Index (LAI) Change Detection Analysis on Loblolly Pine (*Pinus taeda*) Following Complete Understory Removal

J.S. Iiames, R.G. Congalton, A.N. Pilant, and T.E. Lewis

Abstract

*The confounding effect of understory vegetation contributions to satellite-derived estimates of leaf area index (LAI) was investigated on two loblolly pine (*Pinus taeda*) forest stands located in Virginia and North Carolina. In order to separate NDVI contributions of the dominant-codominate crown class from that of the understory, two* P. taeda *1 ha plots centered in planted stands of ages 19 and 23 years with similar crown closures (71 percent) were analyzed for in situ LAI and NDVI differences following a complete understory removal at the peak period of LAI. Understory vegetation was removed from both stands using mechanical harvest and herbicide application in late July and early August 2002. Ikonos data was acquired both prior and subsequent to understory removal and were evaluated for NDVI response. Total vegetative biomass removed under the canopies was estimated using the Tracing Radiation and Architecture of Canopies (TRAC) instrument combined with digital hemispherical photography (DHP). Within-image NDVI change detection analysis (CDA) on the Virginia site showed that the percentage of removed understory (LAI) detected by the Ikonos sensor was 5.0 percent when compared to an actual in situ LAI reduction of 10.0 percent. The North Carolina site results showed a smaller percentage of reduced understory LAI detected by the Ikonos sensor (1.8 percent) when compared to the actual LAI reduction as measured* in situ *(17.4 percent). Image-to-image NDVI CDA proved problematic due to the time period between the Ikonos image collections (2.5 to 3 months). Sensor and solar position differences between the two collections, along with pine LAI increases through multiple needle flush, exaggerated NDVI reductions when compared to in situ data.*

Introduction

Assessment of forest stand-level attributes has been required for the parameterization of many process-based ecological models. Specifically, the leaf surface area has been identified as the main surface of exchange between the plant canopy and the atmosphere and has been related to canopy interception; transpiration; net photosynthesis; gas, water, carbon, and energy exchange; net primary productivity (NPP); biomass; rainfall interception; and dry deposition (Gholz, 1982; Pierce and Running, 1988; Chason *et al.*, 1991; Gower and Norman, 1991; Aber, 2001; Hall *et al.*, 2003). Leaf surface area has been quantified in the ratio of leaf area to ground surface area, a ratio termed the leaf area index (LAI). LAI has been defined here as one-half the total green leaf area per unit ground surface area (Chen and Black, 1992a).

LAI has been estimated from remote sensing satellites using empirical relationships between ground-estimated LAI and vegetation indices derived from primary spectral bands, especially the red and the near-infrared (NIR) wavelengths, taking advantage of the red-edge phenomenon existent within photosynthetically active vegetation (Chen *et al.*, 2002; Lee *et al.*, 2004; Schlerf *et al.*, 2005). The contrast between the visible and the NIR wavelengths forms a strong step in the electromagnetic spectrum of green vegetation between 680 and 750 nm that is often referred to as "the red edge." Many vegetation indices are predicated on this vegetative feature determined by leaf reflectance and transmittance properties, both which are affected by leaf pigments, internal scattering, and leaf water content (Gates *et al.*, 1965; Gausmann *et al.*, 1969; Myers, 1970; Peterson and Running, 1989; Jensen, 2000). Healthy vegetation absorbs approximately 80 percent of incoming solar radiation in the red and blue portions of the spectrum based on the presence of leaf pigments in the palisade mesophyll. However, scattering occurs in the NIR portion of the spectrum due to the presence of spongy mesophyll. The effect of this morphological characteristic may cause upwards of 76 percent scattering of the incoming solar radiation in the 700 to 1,200 nm region (Jensen, 2000).

The exploitation of this vegetative red-edge characteristic in remote sensing applications is tempered by the issue of saturation where an asymptotic increase in a vegetation index (VI) occurs with increasing LAI. The root of the LAI saturation problem with respect to satellite vegetation indices hinges on (a) leaf level differences (e.g., pigments, internal leaf structure, leaf orientation) (Baret and Guyot, 1991; Williams, 1991; Bouman, 1992; Yoder and Waring, 1994), (b) within tree

J.S. Iiames and A.N. Pilant are with the U.S. Environmental Protection Agency, 109 T.W. Alexander Drive, MD E243-05, RTP, NC 27709 (iiames.john@epa.gov).

R.G. Congalton is with the University of New Hampshire, Durham, NH.

T.E. Lewis is with the U.S. Army corps of Engineers, Vicksburg, MS.

Photogrammetric Engineering & Remote Sensing
Vol. 74, No. 11, November 2008, pp. 1389–1400.

0099-1112/08/7411–1389/$3.00/0

crown differences (e.g., clumping and woody material contribution to total reflectance) (Williams, 1991; Huemmrich and Goward, 1997), and (c) differences in canopy level parameters (e.g., tree height heterogeneity and the size and number of tree gaps) (Cohen *et al.*, 1990; Cohen and Spies, 1992; Leblon *et al.*, 1996). The effect of the LAI saturation issue is seen in the poor correlations ($R^2 = 0.30$ to 0.52) reported between the normalized difference vegetation index (NDVI) and LAI (Spanner *et al.*, 1990; Nemani *et al.*, 1993; Chen and Cihlar, 1996). A variety of influences contribute to the poor correlations observed in the LAI-NDVI relationship, namely canopy closure, background materials (i.e., soil properties and soil moisture content), and understory contributions. Of the above mentioned three factors, canopy closure has been identified as the most important variable in determining canopy reflectance regardless of the understory component, due to the masking (i.e., occlusion of understory and ground cover) properties at varying canopy closure values (Spanner *et al.*, 1990; Stenback and Congalton, 1990; Danson and Curran, 1993). However, in forests stands where direct solar radiation is relatively non-occluded (LAI <3), the contribution of understory vegetation has been shown to dramatically increase the NIR reflectance from conifer stands (Nemani *et al.*, 1993) thus affecting the overall response of NDVI.

Understory vegetation may contribute up to 60 percent of total stand LAI, yet detection of this component by various remote sensing platforms/sensors has been difficult due to a variety of influences on overall spectral behavior (i.e., seasonality, canopy structure, image scene dependency, etc.). Chen (1996) reported that the effective LAI (L_e), a canopy attribute influenced by the "effect" of nonrandom foliage spatial distribution on indirect measurements of LAI, varied by less than 5 percent in boreal conifer stands from spring to summer, however the red/NIR Ratio, or Simple Ratio (SR), changed dramatically from spring to summer due to the growth of the understory. This response is a result of the dramatic influence of hardwood understory to the overall NIR reflectance from conifer forests. On average, understory accounted for approximately 20 percent of the total LAI in both old growth ponderosa pine and young ponderosa pine regeneration (Law *et al.*, 2001). Understory LAI accounted for 35 to 60 percent of the total LAI within plots of naturally regenerated young trees (Law *et al.*, 2001). The broadleaved component in the understory with a conifer overstory showed a large effect in the NIR, a moderate effect in the red, and, little to no effect in the shortwave IR regions (Peterson and Running, 1989). Badhwar *et al.*, (1986) found that understory NIR reflectance dominated overall reflectance from open-canopied stands.

Separating the spectral signal from multi-layered forest canopies, especially those with a significant presence of understory, has proven difficult in the assessment of LAI in those forest stands (Franklin *et al.*, 1997; Carlson and Ripley, 1997). We investigated the confounding effect of understory contributions to satellite-derived estimates of LAI on two loblolly pine (*Pinus taeda*) plantations (ages 19 and 23 years) located in Virginia and North Carolina, USA. Understory vegetation was removed from 1-hectare (ha) plots (100 m × 100 m) within both stands using mechanical harvest and herbicide application in late July and early August 2002. Ikonos multispectral imagery was collected both prior and subsequent to understory removal and was evaluated for change in VI response in the harvested and non-harvested areas. LAI change, a result of the removal of understory vegetation beneath the dominant *P. taeda* canopy, was estimated using an integrated optical LAI estimation technique combining measurements from the Tracing Radiation and Architecture of Canopies (TRAC; 3rd Wave Engineering, Ontario, Canada) instrument with digital hemispherical photography (DHP).

Methods

In situ broadleaf forest understory contributions to overall stand LAI were analyzed on two *P. taeda* sites located in the Albemarle-Pamlico Basin. On these same two sites, a VI change detection analysis was completed using 4 m multi-resolution Ikonos imagery. On both sites, within a 1 ha area, broadleaf understory and ground vegetation were removed using mechanical harvest and herbicide application in late July and early August 2002. Ikonos imagery was acquired pre-(IM-T1) and post-(IM-T2) harvest through the NASA Data Buy Program for analysis (Morisette *et al.*, 2003). *In situ* LAI was measured prior to and following the understory removal implementing the indirect optical estimation method integrating TRAC and DHP measurements (TRAC-DHP). IM-T1 and IM-T2 pair-wise Ikonos images for each site were first georectified then normalized using the localized relative radiometric normalization technique in order to assess change between the two dates (Elvidge *et al.*, 1995). Pair-wise images were then clipped to include the 1 ha site (UR region, i.e., understory removal) plus the unaltered *P. taeda* stand immediately surrounding the site (UA region, i.e., unaltered). VIs using the red edge properties characteristic within photosynthetically active vegetation were utilized to assess LAI change. Comparisons between dates (image-to-image) and within-date (within-image) were made employing low-pass spatial filters at varying resolutions. An analysis of variance (ANOVA) was implemented to test for significant differences between dates (i.e., image-to-image) IM-T1 and IM-T2. A within-date (i.e., within-image) ANOVA was applied to test for differences in the IM-T2 image between the 1 ha UR and the UA regions.

Site Descriptions

Two sites chosen for this research were located on commercial forestland managed for pulp and paper production in Virginia and North Carolina. The Virginia (Appomattox) site is located in Campbell County, VA (37.219°N, −78.879 °W) approximately 15.5 km SSW of Appomattox, VA (Figure1). This upper piedmont region ranges in elevation of 165 to 215 m above mean sea level. The MeadWestvaco Corporation, a supporter of the Sustainable Forestry Initiative, permitted sampling access to the U.S. Environmental Protection Agency (EPA) for this *P. taeda* stand including a complete understory removal within the 1 ha UR region using mechanical harvest and herbicide application. *P. taeda* was planted in 1980. Predominant soil types within the county included both Typic Hapludults and Kanhapludults: Cecil (16.3 percent), Cullen (12.0 percent), Tatum (8.3 percent), and Appling (7.7 percent). Measurements of forest structural attributes (height [m] and diameter [cm]) were made at both sites within the 1 ha areas using a point sampling method (nine plots/ha) with a basal-area-factor 10 for trees larger than 5 cm diameter at breast height (DBH) (Avery and Burkhart, 1993). Three plots within both 1 ha UR regions were sampled for understory components (stems less than 5 cm DBH) using a 4.6 m radius fixed area sampling method. Canopy closure, defined as the percent obstruction of the sky by canopy elements, was estimated using a GRS Densitometer (Ben Meadows Co., Janesville, WI). Stocking values, expressed as trees per hectare (TPH), were 1,250 TPH for the dominant-codominant crown class and 3,790 TPH for all trees in the understory (suppressed). The Appomattox understory did not have one dominant species as found in the Hertford site understory, however all tree species were deciduous (Figure 2). The average diameter (DBH), measured 1.4 m above the base of the tree, was 21.6 cm. The average height of the dominant-codominant crown class was 15.9 m. This *P. taeda* stand supported a basal area (BA) per hectare of 36.7 m^2, with BA defined as the cross-sectional

Figure 1. North Carolina (Appomattox) and Virginia (Hertford) *P. taeda* site locations.

area of a tree at 1.4 m above the tree base per unit area. The crown closure was 71 percent for this forest type (Table 1).

The North Carolina (Hertford) site, located in Hertford County, NC (36.383°N, −77.001°W), is approximately 5.8 km WSW of Winton, NC (Figure 1). This coastal plain site is 8 to 10 m above mean sea level with a moderately well drained thermic Aquic Hapludult soil type (Craven fine sandy loam). *P. taeda* was planted in 1983 and by

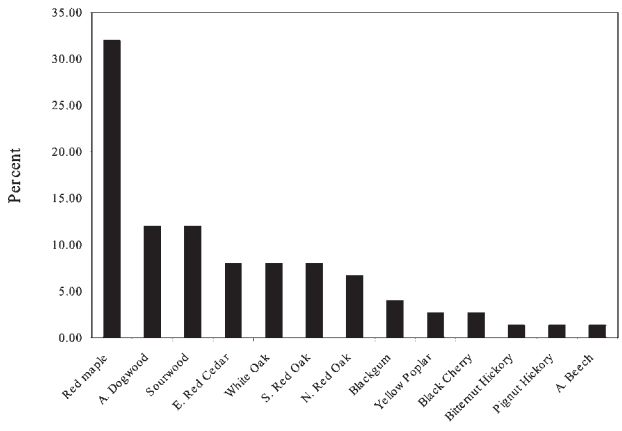

Figure 2. Distribution of understory (percent Stems/ha) tree species sampled on the Appomattox site.

TABLE 1. FOREST STAND STRUCTURE ATTRIBUTES FOR APPOMATTOX (VA) AND HERTFORD (NC)

	Appomattox	Hertford
TPH (overstory)	1250	1740
TPH (understory)	3790	2830
STAND AGE (years)	23	19
DBH (cm)	21.6	18.5
HEIGHT (m)	15.9	14.3
BA/H (m^3)	36.7	37.3
CC (%)	71	71

2002 stocking values were 1,740 TPH for the dominant-codominant canopy class and 2,830 TPH for the suppressed canopy crown class. Understory was dominated (60 percent) by the broadleaf evergreen tree species *Ilex opaca* (American Holly) (Figure 3). The average diameter and height of this stand was 18.5 cm and 14.3 m, respectively. Measured basal area and crown closure was 37.3 m^2/ha and 71 percent, respectively (Table 1).

Understory Harvest and Herbicide Application

Understory removal completion dates were 30 July 2002 (Hertford) and 02 August 2002 (Appomattox). The perimeters of both 100 m × 100 m plots on both sites were flagged and a mechanical harvest was applied, effectively shredding all understory. To ensure elimination of all photosynthetically active vegetation in the understory, including forbs, herbs, and grasses, an herbicide treatment of two quarts/acre of Accord Concentrate (Dow AgroSciences, Indianopolis, IN) was applied to both plots (Plate 1). This understory component was not significant (~10 to 15 percent) given the shading produced by the dominant-codominant and suppressed tree crown classes existent on both sites.

In situ LAI Measurements

A number of LAI validation studies have utilized the integration of optical instruments to capture gap fraction measurements and gap size distributions to estimate L_e and Ω_E. Leblanc and Chen (2001) combined the TRAC with LICOR PCA measurements for *in situ* LAI, as did Jonckheere *et al.* (2005). TRAC-DHP integration LAI estimation was assessed in the *P. taeda* pine forests of North Carolina and Virginia with good correlation to whole-tree harvest LAI estimates (Iiames, 2006). Recently, Ω_E has been extracted from gap size

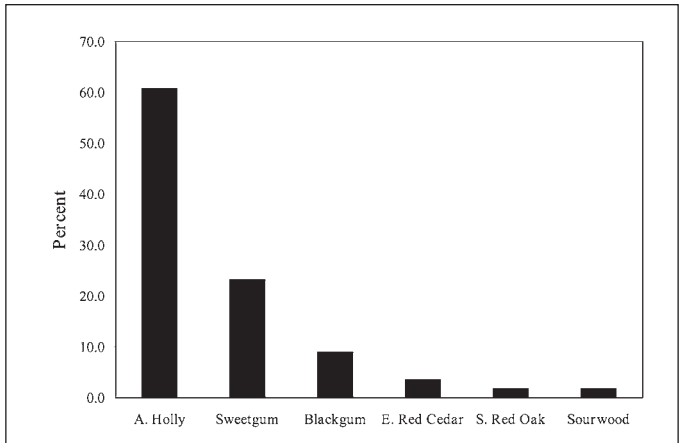

Figure 3. Distribution of understory (percent Stems/ha) tree species sampled on the Hertford site.

(a)

(b)

(c)

Plate 1. Appomattox, Virginia: (a) understory harvest, (b) pre-harvest conditions, and (c) post-harvest conditions.

distribution within DHP measurements, potentially eliminating the requirement of TRAC measurements to obtain the same parameter (Leblanc *et al.*, 2005). However, Chen *et al.* (2006) cautioned against exclusive use of DHP to estimate Ω_E due to (a) the effect of multiple scattering causing a loss of leaf/needle resolution in the vertical direction, and (b) the distortion of the gap size distribution resulting from the loss of these small gaps.

Indirect optical estimation of LAI utilizing the TRAC-DHP method was completed on both sites immediately prior to (i.e., collection 2 [C2]: July 2002) and immediately following (i.e., collection 3 [C3]: August 2002) understory removal. *In situ* LAI change from these measurements would later be contrasted with NDVI change within-image for each site after harvest. In addition to the C2 and C3 LAI estimates, TRAC-DHP measurements were made on the Appomattox site in May 2002 (collection 1 [C1]) in order to assess LAI differences corresponding to the image-to-image NDVI change found during the same period. The TRAC-DHP indirect optical estimation method employs an equation (Equation1) developed by Chen (1996) based on the Beer-Lambert (Beer, 1853) light extinction model, taking into account that the total amount of radiation intercepted by a canopy layer is dependent on the incident irradiance, canopy structure and optical properties of the site (Jonckheere *et al.*, 2005). This equation (modified Beer-Lambert light extinction model) solves for true LAI and is defined:

$$\mathrm{LAI} = (1 - \alpha) \cdot [L_e(\lambda_E/\Omega_E)], \tag{1}$$

where LAI is the leaf area index representing one-half of the total leaf area per unit ground surface area, α is the woody-to-total area ratio, L_e is the effective LAI, λ_E is the needle-to-shoot area ratio, and Ω_E is the element clumping index. In summary, the effective LAI, L_e, is estimated from DHP gap fraction measurements; the element clumping index, Ω_E, is calculated from gap size distributions determined from TRAC measurements; the woody-to-total area and needle-to-shoot area ratios are calculated using a combination of field and laboratory methods.

The TRAC sunfleck-profiling instrument consists of three quantum photosynthetically active radiation (PAR) (400 to 700 nm) sensors (LICOR, Lincoln, NE, Model LI-190SB), two uplooking and one downlooking, mounted on a wand with a built-in datalogger (Leblanc *et al.*, 2002). The instrument is hand-carried approximately 1 m above the ground in direct sun conditions along a linear transect at a constant speed of 0.3 m/s. Typical transect lengths of 50 m to 100 m or greater are oriented close to perpendicular to the direction of the sun and are marked in fixed intervals, typically 10 m subdivisions. A user-defined time stamp initiates the transect collection with each intermediate 10 m subdivision also marked by the user progressing along the transect. The instrument records the downwelling solar photosynthetic photon flux density (PPFD) from one of the uplooking sensors in units of μmol/m^2/s at a sampling frequency of 32 HZ. The datalogger records light-dark transitions as the direct solar beam is alternately transmitted and eclipsed by canopy elements. A 30° to 60° solar zenith angle (θ) is recommended for TRAC measurements in order to process gap fraction. TRAC data are processed by TRACWin software (Leblanc *et al.*, 2002) to yield the element clumping index (Ω_e) from the deviation of the measured gap size distribution from that of randomly distributed foliage (Morisette *et al.*, 2006).

DHP measurements were made with a Nikon CoolPix 995 digital camera with a Nikon FC-E8 fish-eye converter in diffuse light conditions. An image size of 1,600 pixels $\times$ 1,200 pixels was selected at an automatic exposure. The camera was mounted on a tripod and was leveled over each stake at a height of 1.4 m using a combination of two bubble levelers, one on the tripod and one mounted on the lens cap. Proper leveling of the instrument ensured that the "true" horizon of the photograph was captured. The camera was oriented to true north in order to compare

metrics derived from other canopy gap instruments (e.g., TRAC, densitometer, etc.). The operator would select a delayed (3 to 10 second) exposure to eliminate any vibration incurred when depressing the shutter.

Gap Light Analyzer (GLA) software (Simon Fraser University, Burnaby, British Columbia, Canada) was used to process the DHP imagery. GLA relies on the accurate projection of a three-dimensional hemispherical coordinate system onto a two-dimensional surface. After downloading the images, a GLA configuration file was created for both sites. A configuration file contains information regarding image orientation, projection distortion and lens calibration, site location coordinates, length of growing season, sky-region brightness, and atmospheric conditions. GLA requires that each image be registered with respect to the location of due north on the image and the image circular area. This image registration process required that the FC-E8 fish-eye lens be recalibrated due to an actual field of view of 185°, not 180°. The image radius was reduced accordingly so that the 90°θ represented the true horizon. After the image was registered, an analyst-derived threshold value was assigned, delineating sky (white pixels) from no-sky (black pixels). GLA software returns gap fraction values for the following θ's: 5.6°, 16.9°, 28.1°, 39.4°, 50.6°, 61.9°, 73.1°, and 84.4°. Miller (1967) found that gap fraction measurements made at 1 radian (~57.3°) for a variety of leaf or needle structures converge at a 0.5 projection coefficient (Beer-Lambert variable). This theoretical insensitivity of gap fraction to leaf angle distribution at 57.3° eliminates the requirement for gap fraction measurements over the entire range of θ's. The gap fraction at 57.3° can be determined by plotting gap fraction values against the corresponding θ's. Solving for L_e from the Beer-Lambert equation results in:

$$L_e = \ln P(\theta)\,(-2\cos(\theta)) \quad (2)$$

where $P(\theta)$ is the gap fraction at θ.

The needle-to-shoot area (γ_E) and woody-to-total area (α) ratios were measured from samples taken from two additional sites located within the same physiographic provinces as the Appomattox and Hertford sites. The needle-to-shoot area ratio was obtained through laboratory analysis of shoot samples following the methodology of Chen and Black (1992a and b) and Fassnacht *et al.* (1994). The woody-to-total area ratio was estimated using ERDAS Imagine® image processing software through an unsupervised classification technique employing the ISODATA clustering algorithm (Iiames, 2006).

Sample Design

The primary sampling unit was the quadrant, a 100 m × 100 m grid with five 100 m east-west TRAC sampling transects, labeled line 1 (L1) through line 5 (L5). The east-west grid layout aligned TRAC transects diagonal to the planted rows within both conifer sites, thereby minimizing the impact of clumping (Breda, 2003). Interspersed among the TRAC transects were five DHP transects (lines A through E; Figure 4). Quadrants were designed to approximate a Landsat ETM+ 3 pixel × 3 pixel window. Quadrants on both sites were randomly selected within an area that allowed a 50 m minimum buffer to any road or open areas. The TRAC transect L1_0 m position was located using real-time (satellite) differentially corrected GPS to a horizontal accuracy of ±1.0 m. From this point, TRAC transects were staked every 10 m with pre-labeled 18-inch plastic stakes. The stakes were used in TRAC measurements as walking-pace and distance markers. DHP transects were staked at the 10, 30, 50, 70, and 90 m positions located between the TRAC transects.

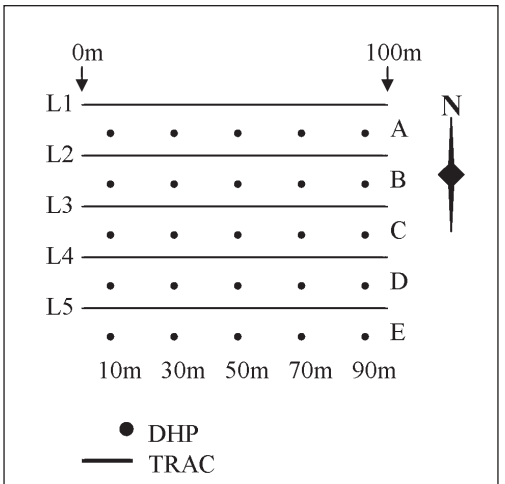

Figure 4. 100 m × 100 m (1 ha) quadrant design.

Ikonos Image Processing

High-resolution (4 m) 11-bit Ikonos image pairs (IM-T1 and IM-T2) corresponding to pre- and post-understory harvest conditions were acquired from NASA's Scientific Data Purchase for both sites (Morisette *et al.*, 2003). IM-T1 Appomattox and Hertford images were obtained on 24 May and 12 May 2002, respectively, whereas IM-T2 images were acquired on 03 August (Appomattox) and 13 August (Hertford). Acquisition time occurred within a narrow morning window of 0957 to 1032 (UTC), with collection azimuth differing significantly (123.3°) between dates for both sites (Figure 5). Images were geometrically registered (georectified) to 1998 color infrared digital orthophotograph quarter-quadrangles (DOQQ) for both sites using ERDAS Imagine® 8.6 software. Prior to the geometric registration, field ground control points were collected using ±1 m real-time differentially corrected GPS (Omnistar, Houston, TX) and compared to DOQQ locations of the same

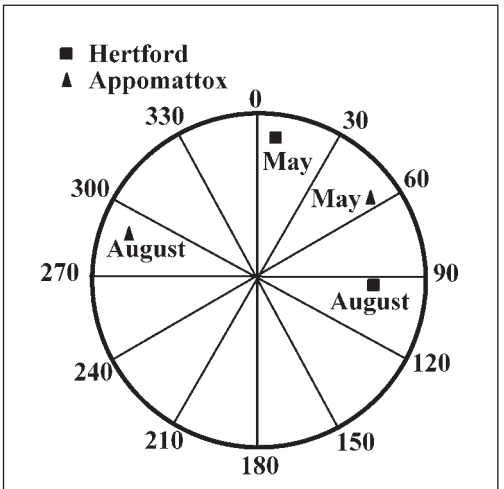

Figure 5. Ikonos collection azimuths from Appomattox image pairs (IM-T1, IM-T2).

point. Offsets in the X and Y direction were assessed for DOQQ accuracy prior to assuming this data layer as the base for georectification.

After the georectification process was completed image analysis was conducted to test: (a) image-to-image NDVI CDA using relative radiometric normalization technique (Appomattox site only), (b) within-image NDVI CDA (Appomattox and Hertford IM-T2 images), (c) spatial averaging unit appropriate for the *P. taeda* forest type, and (d) differences between NDVI and four other vegetation indices.

Image-to-Image NDVI Change Detection Analysis

To test IM-T1 and IM-T2 image-to-image NDVI change detection, the Appomattox image pair was subset to a 37.4 ha area centered about the 1 ha UR region (Plate 2). A relative radiometric normalization using an automatic scattergram-controlled regression was applied to the IM-T2 (August 2002) image in conjunction with the IM-T1 (April 2002) image (Elvidge *et al.*, 1995). Top-of-atmosphere reflectance-based NDVI images were created from these normalized image pairs. The 37.4 ha image pairs were then clipped to a 4.0 ha area completely contained within the *P. taeda* forest type, again centered about the 1 ha UR region. NDVI image subtraction was applied to both normalized images on an averaged 5 pixel by 5 pixel (i.e., 5 × 5 window) basis. This 5 × 5 spatial averaging window was chosen based on the spatial distribution of the trees within the two stands at Hertford and Appomattox. Stocking values of 1,250 TPH (Appomattox) translated into a nominal tree spacing of ±3 m. Thus, a 20 m × 20 m area 5 × 5 window) would theoretically contain 50 trees with the associated gaps, more than ample size to sample the variability within this crown type. NDVI change less than either positive or negative 0.01 was arbitrarily deemed as a "no-change" pixel. Descriptive statistics were generated for both the 1 ha UR and UA regions between the two dates.

Within-Image NDVI Change Detection Analysis (CDA)

To test within-image NDVI change, both site-specific (Appomattox and Hertford) IM-T2 top-of-atmosphere reflectance-based NDVI images were subset to include both the 1 ha UR region and the similar surrounding *P. taeda* forest stand type (UA region). Change and no change was evaluated on an averaged 5 pixel by 5 pixel basis, employing an analysis of variance (ANOVA) to test for differences between the 1 ha UR and UA regions. While this test could be considered as a pseudo-replicated analysis (Hurlbert, 1984), the goal was not to provide an overall test in a formal experimental design, but to explain the difference beyond the pixel-to-pixel variability.

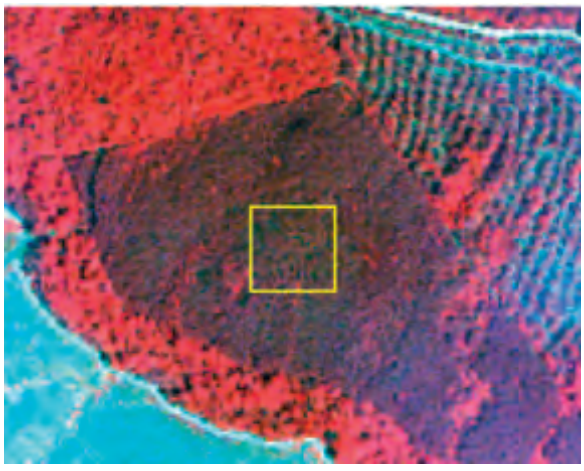

Plate 2. Color infrared subset (37.4 ha) of post harvest image (IM-T2) (Appomattox, Virginia) later normalized to pre-harvest (IM-T1) image. Yellow bounding box is 100 m × 100 m harvested area.

Spatial NDVI Averaging and Testing Other VIs

Spatial NDVI averaging window sizes of 3, 5, 7, and 9 pixels were evaluated on the Hertford IM-T2 image to test for optimal resolution capturing *P. taeda* crown variability. Finally, percent change within the Hertford IM-T2 image was evaluated using the vegetation indices: tNDVI, $\sqrt{(NIR/Red)}$, NIR – Red, and SR.

Results

In situ LAI Measurements

Collections of pre- and post-harvest TRAC measurements (Ω_E) for both sites were designed to acquire PPFD values between the optimal sampling period of 30° to 60° θ. However, due to limited atmospheric conditions (i.e., increased scattered clouds) or time-limited constraints associated with the distance between sites, some TRAC measurements were made outside the preferred 30° to 60° range and, therefore, the preferred time of day. TRAC measurements outside of this optimal θ range might bias Ω_E estimates only if the canopy was highly clumped (i.e., $\Omega_E << 1.0$). However, within these two stands *P. taeda* Ω_E values were close to unity indicating minimal clumping (Leblanc *et al.*, 2005).

For within-image and image-to-image NDVI CDA, three dates of TRAC measurements were made on the Appomattox site (23 May [C1], 30 July [C2], and 05 August [C3] 2002; Table 2). Because only within-image CDA was applied to the Hertford site, only two dates (27 July [C2] and 05 August [C3] 2002) of *in situ* LAI data were collected (Table 2). Corresponding DHP measurements were made on both sites on or within one day of the TRAC measurements within the 100 m × 100 m sampling grid. The woody-to-total area (α = 0.25) and the needle-to-shoot area (γ_E = 1.21) ratios were applied to both sites in the calculation of LAI.

Applying the input parameters into the modified Beer-Lambert light extinction model (i.e., Ω_E (TRAC), L_E (DHP), α, and γ_E), LAI (overstory and understory) was calculated for the three *in situ* collection periods for the Appomattox site (C1 to C3) and the two collection periods for the Hertford site (C2, C3). At the Appomattox site there was a 16.9 percent increase in *in situ* LAI between C1 (LAI = 2.01) and C3 (LAI = 2.35). However, within-image NDVI CDA revealed a 10.0 percent *in situ* LAI reduction between C2 (LAI = 2.61) and C3 (LAI = 2.35) (Table 3). At the Hertford site *in situ* LAI differences between C2 and C3 (within-image NDVI CDA) showed a 17.4 percent reduction (C1 = 2.41 LAI; C2 = 1.99 LAI; Table 3).

Ikonos Image Analysis

Georectification

Mean differences in geolocated GCPs compared to DOQQ points of the same location showed reasonable accuracy for both sites in the both the X and Y direction. The Appomattox site showed a mean deviation in the X and Y directions of 2.36 m and 2.13 m, respectively. The Hertford site showed a mean deviation in the X and Y directions of 2.07 m and 0.53 m, respectively. The georectification process for both sites (IM-T2

TABLE 2. *IN SITU* LAI PARAMETERS FOR APPOMATTOX AND HERTFORD SITES FOR THREE COLLECTION PERIODS (C1-MAY 2002; C2-JULY 2002; C3-AUGUST 2002)

		C1	C2		C3	
		APPO	APPO	HERT	APPO	HERT
	W/IN-IM		X	X	X	X
	IM-IM	X			X	
TRAC	DATE	23 May 2002	30 July 2002	27 July 2002	06 August 2002	05 August 2002
	TIME (UTC)	13:54–14:25	9:13–9:41	11:38–12:18	9:34–9:54	12:59–13:26
	θ	18.9–22.9°	57.0°–51.3°	27.2°–21.1°	53.8°–49.9°	19.8°–19.7°
	S. AZIMUTH	211.6°–228.7°	91.0°–95.6°	122.9°–140.9°	96.3°–99.8°	169.4°–188.6°
	TRANSECTS (D)	L1–5 (W–E)	L1–5 (W–E)	L1–5 (W–E)	L1(10,50,90) (N–S)[1]	L1–5 (W–E)
	PPFD (μmol/m^2/s)	1850–1920	340–1013	585–928	401–668	1345–1416
	$\Omega_E(\sigma)$	0.91 (0.04)	0.89 (0.05)	0.92 (0.03)	0.90 (0.04)	0.89 (0.03)
DHP	DATE	23 May 2002	29 July 2002	25 July 2002	06 August 2002	05 August 2002
	POINTS	A(10,50,90) C(10,50,90) E(10,50,90)	All (A,B,C,D,E)	All (A,B,C,D,E)	B(30,50,70) C(30,50,70) D(30,50,70)	B(30,50,70) C(30,50,70) D(30,50,70)
	$L_E(\sigma)$	1.79 (0.21)	2.25 (0.28)	2.21 (0.28)	2.07 (0.20)	1.78 ((0.10)

Note: TRAC lines were run N-S due to solar position. TRAC runs began at L1_10 then proceeded south through L2, L3, L4, and L5_10. The next TRAC run began at L5_50, then proceeded north along the 50 m markers. The same process was repeated for L1_90, proceeding south.

TABLE 3. CALCULATION OF *IN SITU* LAI (TRAC-DHP) FOR APPOMATTOX (VA) AND HERTFORD (NC) SITES

Site	Collection	Month/Year	Ω_E	L_E	γ_E	α	LAI	[1]ADJ LAI
APPO	C1	MAY 2002	0.91	1.79	1.21	0.25	1.78	2.01
APPO	C2	JULY 2002	0.89	2.25	1.21	0.25	2.30	2.61
APPO	C3	AUGUST 2002	0.90	2.07	1.21	0.25	2.08	2.35
HERT	C2	JULY 2002	0.92	2.21	1.21	0.25	2.13	2.41
HERT	C3	AUGUST 2002	0.89	1.78	1.21	0.25	1.76	1.99

Note: ADJ LAI (i.e., adjusted LAI): LAI estimates were adjusted upward by a factor of 1.132 to adjust for the differences accounted between *in situ* TRAC-DHP estimated LAI and allometrically-derived LAI estimates from destructive harvests (Iiames, 2006).

images) resulted in root mean square error (RMSE) within one-half pixel (i.e., approximately 2 m). RMSE was below one-half pixel for the Hertford site (RMSE = 0.27 m) and close to one-half pixel for the Appomattox site (RMSE = 2.10 m). The IM-T1 images (Appomattox and Hertford) were registered to the corrected IM-T2 images for georectification.

Image-to-Image NDVI Change Detection Analysis

Testing image-to-image NDVI change at both sites was problematic in that the time between the two image dates (IM-T1 and IM-T2) was lengthy (73 days: Appomattox; 94 days: Hertford). Also, the nominal collection azimuths differed within the Appomattox image pairs (236.7°) and the Hertford image pairs (83.8°). Therefore, this method was applied only to the Appomattox image pair to determine if any change could be detected.

The mean UA region NDVI for the IM-T1 (May 2002) image was reduced 9.1 percent between image acquisition dates (Table 4). Within the 1 ha UR region, a 14.3 percent decrease in NDVI was observed between the IM-T1 image and the IM-T2 image. Between-date ANOVA results indicate that there were significant differences between the 1 ha UR ($p = <0.0001$, $F = 1303.9$, $df = 1$) and the UA regions ($p = <0.0001$, $F = 3010.2$, $df = 1$). Within the 1 ha UR region an NDVI image subtraction (pre-harvest image NDVI minus post harvest image NDVI) resulted in 81.2 percent of the area exhibiting a decrease in NDVI greater than 0.01 NDVI change threshold. The remaining 18.8 percent of the 1 ha UR region indicated no change in NDVI. Within the UA region 11.9 percent of the area showed an NDVI decrease (>0.01), 8.5 percent resulted in an NDVI increase (>0.01), and the rest of the area was unchanged.

TABLE 4. IMAGE-TO-IMAGE NDVI CDA (5 × 5 AVERAGED) OF 23 MAY (IM-T1) AND 03 AUGUST 2002 IMAGES (IM-T2) (APPOMATTOX)

	UR (n = 16)			UA (n = 60)		
	5/23/02	8/3/02	% Reduction	5/23/02	8/3/02	% Reduction
μ	0.58	0.49	14.3	0.57	0.52	9.1
σ	0.004	0.004		0.009	0.006	

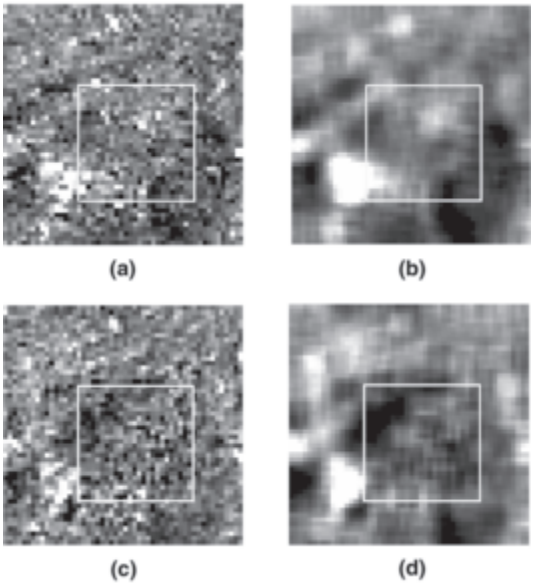

Figure 6. Appomattox 23 May 2002 (IM-T1): (a) NDVI, and (b) 5 × 5 NDVI; Appomattox 03 August 2002 (IM-T2):(c) NDVI, and (d) 5 × 5 NDVI. Note: Darker regions indicate areas of low NDVI.

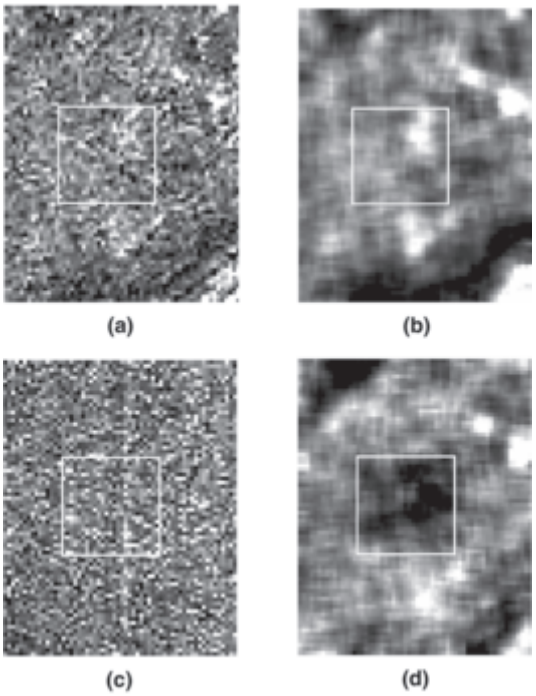

Figure 7. Hertford 12 May 2002 (IM-T1): (a) NDVI, and (b) 5 × 5 NDVI; Hertford 13 August 2002 (IM-T2): (c) NDVI, and (d) 5 × 5 NDVI.

Within-image NDVI Change Detection Analysis

Significant differences were detected between the 1 ha UR and the UA regions within the IM-T2 (Appomattox) NDVI image ($p = <0.0001$, $F = 300.9$, $df = 1$) and the IM-T2 (Hertford) NDVI image ($p = <0.0001$, $F = 30.3$, $df = 1$) (Figures 6 and 7). A 5.0 percent decrease in NDVI was detected between the 1 ha UR and the UA regions of the IM-T2 (Appomattox) NDVI image (UR NDVI = 0.493; UA NDVI = 0.519), whereas only a 1.8 percent decrease was detected between the 1 ha UR and UA regions within the IM-T2 (Hertford) NDVI image (UR NDVI = 0.425; UA NDVI = 0.433; Table 5).

Spatial Averaging Window Size

The mean values between four spatial averaging window sizes (3 × 3, 5 × 5, 7 × 7, and 9 × 9) for both the 1 ha UR and the UA regions were identical (Figure 8). All p-values indicated significant differences in the means for the two regions (UR versus UA) within each window size ($p < 0.001$). Note the random noise associated with image A in Figure 8 that resulted from the 4 m NDVI values occurring over canopy gap areas with no understory vegetation (darker pixels) and other 4 m NDVI values occurring over crown tops (light pixels). The spatial averaging in panels B through E (Figure 8) resolve NDVI decreases at the canopy level.

Other Vegetation Indices

Analysis of the four additional vegetation indices besides NDVI revealed that NDVI and NIR – Red resulted in the detection of the largest change across all four indices (Table 6). The vegetation index tNDVI was the least sensitive detector of change.

TABLE 5. WITHIN-IMAGE NDVI CDA (5 × 5 AVERAGED) OF 03 AUGUST 2002 (IM-T2) (APPOMATTOX) AND 13 AUGUST 2002 (IM-T2) (HERTFORD) IKONOS IMAGERY

	UR	UA	Reduction %
Appomattox	0.493	0.519	5.0
Hertford	0.425	0.433	1.8

Discussion

Understory effects on spectral signal to the sensor are confounded by a number of factors including the spatial distribution of variable illumination conditions (direct sunlight, sunflecks, penumbra, shade) (Miller *et al.*, 1997). For example, in the Boreal Ecosystem-Atmospheric Study (BOREAS), these illumination variables affected VI response dependent on forest stand type when evaluating over seasons and time-of-day (Miller *et al.*, 1997). Gamon *et al.* (2004) suggested that optical signature variability in the boreal conifer forests render LAI derived from VIs into question. It has also been shown that understanding the understory contribution to overall LAI has significance in the evaluation of ecosystem flux data. Ponderosa pine carbon-water interactions as well as Slash pine water and energy exchange have been aided by the assessment of the understory LAI contributions (Williams *et al.*, 2001; Powell *et al.*, 2005).

With our research, the image-to-image NDVI CDA within the Appomattox site did show a larger decrease in NDVI within the 1 ha UR region between image dates (14.3 percent) than did the IM-T2 within-image NDVI decrease between the 1 ha UR and UA regions (5.0 percent). However, the image-to-image processing technique had some underlying issues in that the IM-T1 Ikonos acquisition was 2.5 to 3 months prior to the IM-T2 acquisition. Ikonos acquisition azimuthal differences between the two image dates (123.3°) could affect shadowing and the

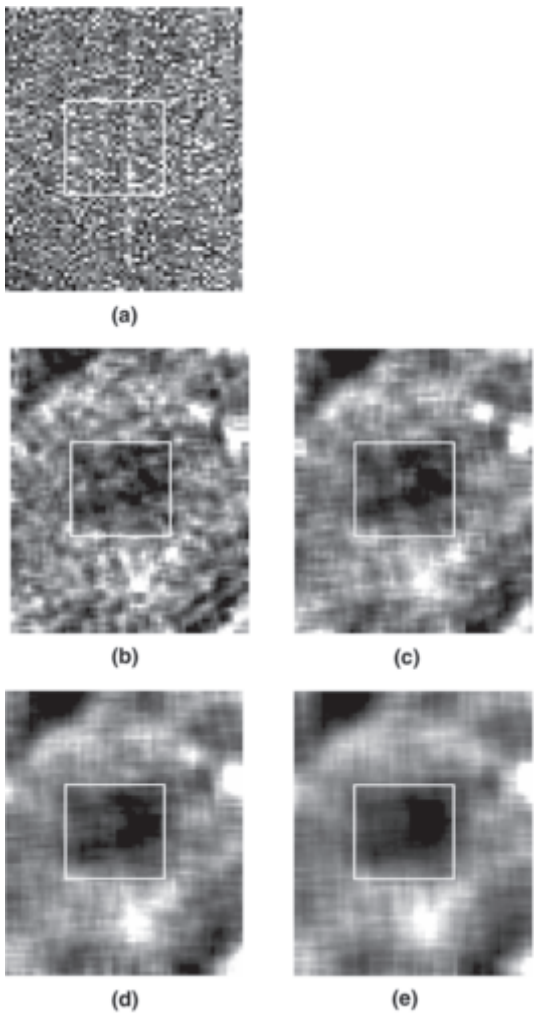

Figure 8. Comparison of various spatial averaging windows on Hertford 13 August 2002 (IM-T2) NDVI image: (a) Raw NDVI, (b) 3 × 3 NDVI, (c) 5 × 5 NDVI, (d) 7 × 7 NDVI, and (e) 9 × 9 NDVI.

amount of NIR reflectance received at the sensor. Also, *P. taeda* incurs tremendous change over the growing season, with the addition of two to three needle flushes common within this species. Sampson *et al.* (2003) found that *P. taeda* LAI varied twofold inter-annually with a minimum LAI in March to April and a maximum in September. This trend is evident when comparing the increase of *in situ* LAI (29.9 percent) from May 2002 (C1), to July 2002 (C2), then the expected decrease (10 percent) between C2 and C3. Viewing only *in situ* LAI change between C1 and C3, an increase of 16.9 percent was recorded, even though significant leaf biomass had been removed (Figure 9). NDVI, contrary to the *in situ* LAI trend, exhibited a continually decreasing tendency between C1 to C2 (9.7 percent), then C2 to C3 (5.0 percent), with an overall NDVI decrease from C1 to C3 of 14.3 percent (Figure 9). Possible explanations for this decrease in NDVI with a corresponding increase *in situ* measured LAI may result from higher NIR reflectivity and red absorption from planophile broadleaf foliage in the understory compared to erectophile foliage typical of conifer needles (Turner *et al.*, 1999) (Table 4). Another possible explanation may be related to the relative visibility of the deciduous understory in the low LAI *P. taeda* conditions typical for the early-late spring period. A direct comparison of empirically-derived LAI, i.e., the correlation of spectral data with *in situ* estimated LAI, and *in situ* LAI was not possible due to the narrow range of LAI values within this stand.

Within-image NDVI CDA compared the 1 ha UR and UA regions for both sites within each corresponding IM-T2 (August 2002) image. Significant differences between both regions (UR and UA) were detected. However, within the 1 ha UR region, the Appomattox and Hertford sites behaved differently with respect to the percent reduction in NDVI and the *in situ* estimated reduction in LAI. The Appomattox site showed a larger decrease in NDVI than the Hertford site within the 1-ha UR regions (5 percent versus 1.8 percent), yet the Hertford site exhibited a greater reduction in LAI (17.4 percent versus 10.0 percent). One possible explanation for this result may be the large percentage of *Ilex*

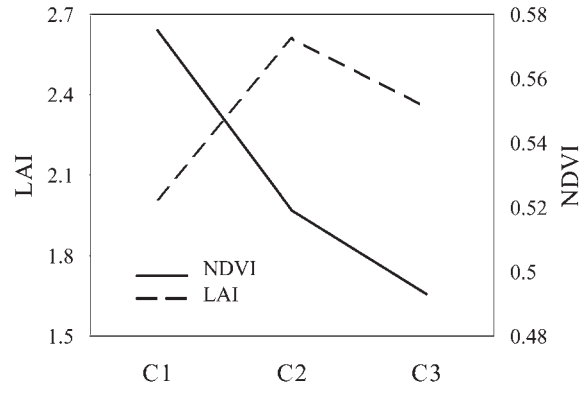

Figure 9. Image-to-image NDVI CDA and *in situ* LAI trends over three collection periods (C1-May 2002; C2-July 2002; C3-August 2002) Appomattox, Virginia.

TABLE 6. VEGETATION INDICES DIFFERENCES EVALUATING BIOMASS CHANGE DETECTION FOR THE 13 AUGUST 2002 (IM-T2) HERTFORD IKONOS NDVI IMAGE (H = HARVESTED; NH = NON-HARVESTED)

	NDVI	tNDVI	NIR/Red	NIR-Red	NIR/Red
	(H:NH)	(H:NH)	(H:NH)	(H:NH)	(H:NH)
μ	0.425:0.433	0.963:0.966	1.580:1.591	401.4:408.8	0.426:0.434
σ	0.004:0.005	0.003:0.002	0.010:0.009	7.79:7.56	0.004:0.004
% Diff	1.80	0.33	0.73	1.80	1.72
p	<0.001	<0.001	<0.001	<0.001	<0.001

opaca (American Holly) existent within the Hertford understory (60 percent). This species is extremely shade tolerant, thus exhibits characteristics typical of this shade class (increased photosynthetic and respiratory efficiency, increased light use efficiency, and, increased leaf surface area). There is a visible difference between the leaf underside and top of leaf. The non-Lambertian surface (leaf and canopy) could produce significantly spectral differences dependent on the image acquisition angle. In addition to the *Ilex opaca* issue, returned reflectance to the sensor may further have been reduced by the larger presence of organic soils in this coastal plain site compared to the piedmont site (Appomattox).

The question arises on how other sensor-derived NDVI might detect subtle changes in forest stand structure. Spectral vegetation indices may not be comparable due to sensor spectral and spatial characteristics (Hill and Aifadopoulou, 1990; Teillet *et al.*, 1997; Steven *et al.*, 2003; Soudani *et al.*, 2006). The primary issue affecting NDVI differences between sensors was the spectral characteristic of the red band (i.e., width, location) (Teillet *et al.*, 1997; Soudani *et al.*, 2006). Ikonos-derived NDVI was observed to be systematically lower than Landsat ETM+ -and SPOT HRVIR-derived NDVI, with an observed offset approximately 0.11 and 0.20 NDVI units dependent on image preprocessing techniques (i.e., atmospheric corrections) (Soudani *et al.*, 2006). No generalized Ikonos NDVI-LAI regression model was found in the literature for *P. taeda* in the southeastern U.S. However, a general comparison was made between within-image Ikonos-derived NDVI change observed on both sites and retrieved NDVI differences from a species-specific nonlinear regression model developed from the HyMap (Integrated Spectronics Pty Ltd., 1997) sensor (Flores, 2003). This equation was developed by regressing *in situ* estimated LAI with HyMap-retrieved NDVI on two *P. taeda* stands located in the North Carolina Sandhills and Coastal Plain regions. Flores (2003) found this equation to be transferable across sites, stand structures, and seasons. By applying C2 and C3 *in situ* LAI estimates into the Flores regression model, predicted NDVI values were retrieved for both the Appomattox and Hertford sites. The HyMap NDVI was shown to be 0.21 (Appomattox) and 0.28 (Hertford) NDVI units above those observed with the Ikonos sensor, values similar to differences observed between the Landsat ETM+ and SPOT HRVIR sensors. Results were indifferent as to which sensor might have more appropriate detection abilities. On the Appomattox site, a 2.8 percent NDVI reduction was predicted by the Flores regression model as compared to a larger NDVI reduction (5.0 percent) observed with the Ikonos-derived NDVI. On the other site, the Flores regression model predicted a larger NDVI reduction than that observed with Ikonos sensor (5.0 percent versus 1.8 percent). It would be expected that, if available, actual observed HyMap-derived NDVI values would be more highly detectable due to the higher spectral resolution and the corrections for atmospheric interference.

The 5×5 spatial averaging window was chosen to offset issues inherent within higher spatial resolution sensors: (a) the introduction of heterogeneity at a finer scale than that from which *in situ* LAI is measured, and (b) the resolving of canopies at the individual tree level (Cohen *et al.*, 1990; Turner *et al.*, 1999). Regarding the comparison of the various VIs, NDVI detected the most change in biomass compared to the other four indices. Both sites had yet to reach the asymptotic point in the NDVI-LAI relationship; thus, the relationship was described as linear. However, the SR vegetation index may be more useful in areas of higher biomass due to the linear relationship with LAI (Flores, 2003).

Conclusions

Appomattox results showed that the percentage of removed understory detected by the Ikonos sensor in a piedmont site was 5.0 percent when compared to an actual *in situ* LAI reduction of 10.0 percent. The Hertford results showed that a larger percentage of NDVI change was undetected by the Ikonos sensor (1.8 percent) when compared to the actual LAI reduction as measured *in situ* (17.4 percent). Possible reasons for these differences may be based upon underlying soil types (organic) and/or bi-directional reflectance distribution functions for the non-Lambertian *Ilex opaca* canopy. Off-nadir image acquisitions for both sites would inhibit view of understory conditions for both sites (solar elevation $\approx 65°$).

Acknowledgments

The authors wish to express their gratitude to Jerry Hansen of International Paper Corporation and Vick Ford of Mead-Westvaco who facilitated access to the Appomattox and Hertford sites. Ikonos imagery was provided through the NASA Data Buy Program managed by Jeff Morisette and Jaime Nickeson. In addition, John Duncan, Malcolm Wilkins, Milton Bowen, and Govind Gawdi provided network and logistical support. Administrative, statistical, and technical support was given by John Lyon, L. Dorsey Worthy, Ross Lunetta, David Holland, Megan Mehaffey, Jayantha Ediriwickrema, and Joe Knight. Lastly, we would like to thank three anonymous reviewers who provided input to this article as well as the UNH Dissertation Committee who critiqued the initial study design and results: John D. Aber, Mark J. Ducey, Mary E. Martin, and M.L. Smith. The U.S. Environmental Protection Agency funded and conducted the research described in this paper. It has been subject to the Agency's programmatic review and has been approved for publication. Mention of any trade names or commercial products does not constitute endorsement or recommendation for use.

References

Aber, J.D., and J.M. Melillo, 2001. *Terrestrial Ecosystems*, Academic Press, San Diego, California, 556 p.

Avery, T.E., and H. Burkhart, 1993. *Forest Measurements*, New York, McGraw Hill Text, 331 p.

Baret, F., and G. Guyot, 1991. Potentials and limits of vegetation indices for LAI and APAR assessment (absorbed photosynthetically active radiation), *Remote Sensing of Environment*, 35:161–173.

Beer, A., 1853. *Einleitung in die höhere Opt*ik, Vieweg und Sohn, Braunschweig, Germany, 430 p.

Badhwar, G.D., R.B. MacDonald, F.G. Hall, and J.G. Carnes, 1986. Spectral characterization of biophysical characteristics in a boreal forest: relationship between Thematic Mapper band reflectance and leaf area index for aspen, *IEEE Transactions on Geoscience and Remote Sensing*, GE-24:322–326.

Bouman, B.A., 1992. Accuracy of estimating the leaf area index from vegetative indices derived from crop reflectance characteristics, A simulation study, *International Journal of Remote Sensing*, 13:3069–3084.

Breda, N.J.J., 2003. Ground-based measurements of leaf area index: A review of methods, instruments and current controversies, *Journal of Experimental Botany*, 54(392):2403–2417.

Carlson, T.N., and D.A. Ripley, 1997. On the relation between NDVI, fractional vegetation cover and leaf area index, *Remote Sensing of Environment*, 62:241–252.

Chason, J.W., D.D. Baldocchi, and M.A. Huston, 1991. A comparison of direct and indirect methods for estimating forest canopy leaf area, *Agricultural and Forest Meteorology*, 57:107–128.

Chen, J.M., and T.A. Black, 1992a. Defining leaf-area index for non-flat leaves, *Plant Cell and Environment*, 15(4):421–429.

Chen, J.M., and T.A. Black, 1992b. Foliage area and architecture of plant canopies from sunfleck size distributions, *Agricultural and Forest Meteorology*, 60:249–266.

Chen, J.M., and J. Cihlar, 1996. Retrieving leaf area index of boreal conifer forests using Landsat TM images, *Remote Sensing of Environment*, 55:153–162.

Chen, J.M., 1996. Optically-based methods for measuring seasonal variation of leaf area index in boreal conifer stands, *Agricultural and Forest Meteorology*, 80:135–163.

Chen, J.M., G. Pavlic, L. Brown, J. Cihlar, S.G. Leblanc, H.P. White, R.J. Hall, D.R. Peddle, D.J. King, J.A. Trofymow, E. Swift, J. Vander Sanden, and P.K.E. Pellikka, 2002. Derivation and validation of Canada-wide coarse-resolution leaf area index maps using high-resolution satellite imagery and ground measurements, *Remote Sensing of Environment*, 80:165–184.

Chen, J.M., A. Govind, O. Sonnentag, Y. Zhang, A. Barr, and B. Amiro, 2006. Leaf area measurements at Fluxnet-Canada forest sites, *Agricultural and Forest Meteorology*, 140:257–268.

Cohen, W.B., T.A. Spies, and G.A. Bradshaw, 1990. Semivariograms of digital imagery for analysis of conifer canopy structure, *Remote Sensing of Environment*, 34:167–178.

Cohen, W.B., and T.A Spies, 1992. Estimating structural attributes of Douglas-fir/western hemlock forest stands from Landsat and SPOT imagery, *Remote Sensing of Environment*, 41:1–17.

Danson, F.M., and P.J. Curran, 1993. Factors affecting the remotely sensed response of coniferous forest plantations, *Remote Sensing of Environment*, 43:55–65.

Elvidge, C.D., D. Yuan, R.D. Weerackoon, and R. Lunetta, 1995. Relative radiometric normalization of Landsat Multispectral Scanner (MSS) data using an automatic scattergram-controlled regression, *Photogrammetric Engineering & Remote Sensing*, 61(11):1255–1260.

Fassnacht, K.S., S.T. Gower, J.M. Norman, and R.E. McMurtrie, 1994. A comparison of optical and direct methods for estimating foliage surface area index in forests, *Agricultural and Forest Meteorology*, 71:183–207.

Flores, F., 2003. *Using Remote Sensing Data to Estimate Leaf Area Index and Foliar Nitrogen of Loblolly Pine Plantations*, Ph.D. dissertation, North Carolina State University, Raleigh, North Carolina, 115 p.

Franklin, S.E., M.B. Lavigne, M.J. Deuling, M.A. Wulder, and E.R. Hunt, 1997. Estimation of forest leaf area index using remote sensing and GIS for modelling net primary production, *International Journal of Remote Sensing*, 18(16):3459–3471.

Gamon, J.A, K.F. Huemmrich, D.R. Peddle, J. Chen, D. Fuentesa, F.G. Hall, J.S. Kimball, S. Goetz, J. Gug, K.C. McDonald, J.R. Miller, M. Moghaddamh, A.F. Rahman, J.L. Roujean, E.A. Smith, C.L. Walthall, P. Zarco-Tejadan, B. Hui, R. Fernandes, and J. Cihlar, 2004. Remote sensing in BOREAS: Lessons learned, *Remote Sensing of Environment*, 89(2):139–162.

Gates, D.M., J.J. Keegan, J.C. Schleter, and V.R. Weidner, 1965. Spectral property of plants, *Applied Optics*, 4(1):11–20.

Gausmann, H.W., W.A. Allen, and R. Cardenas, 1969. Reflectance of cotton leaves and their structure, *Remote Sensing of Environment*, 1:110–122.

Gholz, H.L., 1982. Environmental limits on above-ground net primary production, leaf-area, and biomass in vegetation zones of the Pacific Northwest, *Ecology*, 63(2):469–481.

Gower, S.T., and J.M. Norman, 1991. Rapid estimation of leaf-area index in conifer and broad-leaf plantations, *Ecology*, 72(5):1896–1900.

Hall, R.J., D.P. Davidson, and D.R. Peddle, 2003. Ground and remote estimation of leaf area index in Rocky Mountain forest stands, Kananaskis, Alberta, *Canadian Journal of Remote Sensing*, 29(3):411–427.

Hill, J., and D. Aifadopoulou, 1990. Comparative analysis of Landsat-5 TM and SPOT HRV-1 data for use in multiple sensor approaches, *Remote Sensing of Environment*, 34:55–70.

Huemmrich, K.F., and S.N. Goward, 1997. Vegetation canopy PAR absorbance and NDVI and assessment for ten tree species with the SAIL model, *Remote Sensing of Environment*, 61:254–269.

Hurlbert, S.H., 1984. Pseudoreplication and the design of ecological field experiments, *Ecological Monographs*, 54:187–211.

Iiames, J.S., 2006. *Assessing the Accuracy of the MODIS LAI 1-KM Product in Southeastern United States Loblolly Pine Plantations: Accounting for Measurement Variance from Ground to Satellite*, Ph.D. dissertation, University of New Hampshire, Durham, New Hampshire, 184 p.

Jensen, J.R., 2000. *Remote Sensing of the Environment: An Earth Resource Perspective*, Prentice-Hall, Upper Saddle River, New Jersey,. 544 p.

Jonckheere, I., B. Muys, and P. Coppin, 2005. Allometry and evaluation of in situ optical LAI determination in Scots pine: a case study in Belgium, *Tree Physiology*, 25:723–732.

Law, B.E., S. Van Tuyl, A. Cescatti, and D.D. Baldocchi, 2001. Estimation of leaf area index in open-canopy ponderosa pine forests at different successional stages and management regimes in Oregon, *Agricultural and Forest Meteorology*, 108:1–14.

Leblon, B., L. Gallant, and H. Grandberg, 1996. Effects of shadowing types on ground-measured visible and nearinfrared shadow reflectances, *Remote Sensing of Environment*, 58:322–328.

Leblanc, S.G., and J.M. Chen, 2001. A practical scheme for correcting multiple scattering effects on optical LAI measurements, *Agricultural and Forest Meteorology*, 110:125–139.

Leblanc, S.G., J.M. Chen, and M. Kwong, 2002. *Tracing Radiation and Architecture of Canopies. TRAC Manual*, version 2.1.3., Natural Resources Canada, Canada Centre for Remote Sensing, Ottawa, Ontario, Canada, 25 p.

Leblanc, S., J.M. Chen, R. Fernandes, D.W. Deering, and A. Conley, 2005. Methodology comparison for canopy structure parameters extraction from digital hemispherical photography in boreal forests, *Agricultural and Forest Meteorology*, 129:187–207.

Lee, K.-S., W.B. Cohen, R.E. Kennedy, T.K. Maiersperger, and T. Gower, 2004. Hyperspectral versus multispectral data for estimating leaf area index in four different biomes, *Remote Sensing of Environment*, 91:508–520.

Miller, J.B., 1967. A formula for average foliage density, *Australian Journal of Botany*, 15:141–144.

Miller J.R., H.P. White, J.M. Chen, D.R. Peddle, G. Mcdermid, R.A. Fournier, P. Shepherd, I. Rubinstein, J. Freemantle, R. Soffer, and E. Ledrew, 1997. Seasonal change in understory reflectance of boreal forests and influence on canopy vegetation indices, *Journal of Geophysical Research*, 102(d24):29,475–29,482.

Morisette, J.T., J.E. Nickeson, P. Davis, Y.J. Wang, Y.H. Tian, C.E. Woodcock, N. Shabanov, M. Hansen, W.B. Cohen, D.R. Oetter, and R.E. Kennedy, 2003. High spatial resolution satellite observations for validation of MODIS land products: IKONOS observations acquired under the NASA Scientific Data Purchase, *Remote Sensing of Environment*, 88:100–110.

Morisette, J.T., F. Baret, J.L. Privette, R.B. Myneni, J. Nickeson, S. Garrigues, N. Shabanov, M. Weiss, R. Fernandes, S. Leblanc, M. Kalacska, G. Sánchez-Azofeifa, M. Chubey, M.B. Rivard, P. Stenberg, M. Rautiainen, P. Voipio, T. Manninen, A. Pilant, T. Lewis, J. Iiames, R. Colombo, M. Meroni, L. Busetto, W. Cohen, D. Turner, E. Warner, G.W. Petersen, G. Seufert, and R. Cook, 2006. Validation of global moderate-resolution LAI Products: A framework proposed within the CEOS land product validation subgroup, *IEEE Transactions of Geoscience and Remote Sensing*, 44(7):1804–1817.

Myers, V.I., 1970. Soil, water, and plant relations, *Remote Sensing with Special Reference to Agriculture and Forestry*, National Academy of Sciences, Washington, D.C., pp. 253–297.

Nemani, R., L. Pierce, and S. Running, 1993. Forest ecosystem processes at the watershed scale: Sensitivity to remotely sensed leaf area index estimates, *International Journal of Remote Sensing*, 14(13):2519–2534.

Peterson, D.L., and S.W. Running, 1989. Applications in forest science and management, *Theory and Application of Optical Remote Sensing* (G. Asrar, editor), Wiley, New York, 429–473 p.

Pierce, L.L., and S.W. Running, 1988. Rapid estimation of coniferous leaf-area index using a portable integrating radiometer, *Ecology*, 69(6):1762–1767.

Powell, T.L., G. Starr, K.L. Clark, T.A. Martin, and H.L. Gholz, 2005. Ecosystem and understory water and energy exchange for a mature, naturally regenerated pine flatwoods forest in north Florida, *Canadian Journal of Forest Research*, 35:1568–1580.

Sampson, D.A., T.J. Albaugh, K.H. Johnsen, H.L. Allen, and S.J. Zarnoch, 2003. Monthly leaf area index estimates from point-intime measurements and needle phenology for *Pinus taeda, Canadian Journal of Forest Research*, 33:2477–2490.

Schlerf, M., C. Atzberger, and J. Hill, 2005. Remote sensing of forest biophysical variables using HyMap imaging spectrometer data, *Remote Sensing of Environment*, 95:177–194.

Soudani, K., C. Francois, G. le Maire, V. Le Dantec, and E. Dufrene, 2006. Comparative analysis of IKONOS, SPOT, and ETM+ data for leaf area index estimation in temperate coniferous and deciduous forest stands, *Remote Sensing of Environment*, 102:161–175.

Spanner, M.A., L.L. Pierce, D.L. Peterson, and S.W. Running, 1990. Remote sensing of temperate coniferous forest leaf area index: The influence of canopy closure, understory vegetation and background reflectance, *International Journal of Remote Sensing*, 11(1):95–111.

Stenback, J.M., and R.G. Congalton, 1990. Using Thematic Mapper imagery to examine forest understory, *Photogrammetric Engineering & Remote Sensing*, 56(9):1285–1290.

Steven, M.D., T.J. Malthus, F. Baret, H. Xu, and M.J. Chopping, 2003. Intercalibration of vegetation indices from different sensor systems, *Remote Sensing of Environment*, 88(4):412–422.

Teillet, P.M., K. Staenz, and D.J. Williams, 1997. Effects of spectral spatial and radiometric characteristics of remote sensing vegetation indices of forested regions, *Remote Sensing of Environment*, 61:139–149.

Turner, D.P., W.B. Cohen, R.E. Kennedy, K.S. Fassnacht, and J.M. Briggs, 1999. Relationships between leaf area index and Landsat TM spectral vegetation indices across three temperate zone sites, *Remote Sensing of Environment*, 70:52–68.

Williams, D.L., 1991. A comparison of spectral reflectance properties at the needle, branch, and canopy level for selected conifer species, *Remote Sensing of Environment*, 35:79–93.

Williams, M., B.E. Law, P.M. Anthoni, and M.A. Unsworth, 2001. Use of a simulation model and ecosystem flux data to examine carbon-water interactions in ponderosa pine, *Tree Physiology*, 21:287–298.

Yoder, B.J., and R.H. Waring, 1994. The normalized difference vegetation index of small Douglas-fir canopies with varying chlorophyll concentrations, *Remote Sensing of Environment*, 49:81–91.

(Received 21 August 2006; accepted 06 February 2007; revised 04 April 2007)